Published in final edited form as:
Mol Ther. 2006 September ; 14(3): 328–335. doi:10.1016/j.ymthe.2006.04.003.

In Vivo Delivery of Recombinant Viruses to the Fetal Murine Cochlea: Transduction Characteristics and Long-Term Effects on Auditory Function

Jeffrey C. Bedrosian[1,2], **Michael Anne Gratton**[2,*], **John V. Brigande**[3,*], **Waixing Tang**[1], **Jessica Landau**[2], and **Jean Bennett**[1,†]

[1]F. M. Kirby Center and Scheie Eye Institute, Department of Ophthalmology, University of Pennsylvania School of Medicine, Philadelphia, PA 19104, USA

[2]Department of Otorhinolaryngology, University of Pennsylvania School of Medicine, Philadelphia, PA 19104, USA

[3]Department of Otolaryngology, Oregon Health & Science University, Portland, OR 97239, USA

Abstract

Congenital hearing deficits can be caused by a variety of genetic and acquired conditions. Complete reversal of deficits in the peripheral auditory system may require delivery of corrective genes to cochlear progenitor cells. We tested delivery of lentivirus and an array of recombinant adeno-associated viral (AAV) serotypes for efficiency and cellular specificity of transgene expression after *in utero* delivery to the developing mouse otocyst. Stability of expression and safety with respect to auditory function were then tested in those vectors that had the most favorable *in utero* cochlear transduction characteristics (AAV2/1, AAV2/8, and lentivirus). AAV2/1 was found to be the optimal vector for *in utero* cochlear gene transfer. It efficiently transduced progenitors giving rise to both inner and outer hair cells and supporting cells and had no adverse effect on cochlear cell differentiation. Further, it had no pathological effect on differentiated hair cells or the integrity of the auditory nerve or brain-stem nuclei as measured by auditory brain-stem response testing. AAV2/1 promises to be useful in further studies evaluating differentiation pathways of cochlear cells in health and disease and for developing gene-based therapies for congenital and acquired forms of peripheral hearing loss.

Keywords

adeno-associated virus; hearing loss; cochlea; mouse model; gene transfer; *in utero* therapy; hair cells

[†]To whom correspondence and reprint requests should be addressed at 309C Stellar-Chance Labs, 422 Curie Boulevard, Philadelphia, PA 19104-6069, USA. Fax: +1 215 573 7155. jebennet@mail.upenn.edu.
[*]These authors contributed equally to this work.

Appendix A. Supplementary Data: Supplementary data associated with this article can be found, in the online version, at doi:10.1016/j.ymthe. 2006.04.003.

Introduction

Cochlear gene transfer in adult guinea pigs, mice, and other animals has shown promise as a potentially effective therapeutic modality for the treatment of hearing loss [1]. Developmental abnormalities of the cochlea involving the sensory hair cells may lead to congenital hearing loss and it would be difficult if not impossible to correct these developmental defects through treatment of mature cells. To address this problem, we developed and optimized a method of *in utero* gene transfer into the otocyst of the developing mouse embryo. This approach targets the prosensory progenitor cells of the otocyst, which subsequently differentiate into either hair cells or supporting cells [2].

The transduction characteristics of many different viral vectors have been evaluated *in vivo* in the adult cochlea. These vectors include adenovirus [3], adeno- associated virus (AAV) [4], lentivirus [5], herpes simplex type I virus, and vaccinia virus [6,7]. For the present study, we selected AAV and lentivirus due to their favorable immunologic and therapeutic features with respect to neural tissue. In the adult guinea pig cochlea, AAV2-mediated transgene expression has been demonstrated 24 weeks postinjection [8] without evidence of ototoxicity (as measured by distortion product otoacoustic emissions responses) [9,10]. The AAV serotype 2 genome (i.e., AAV2 inverted terminal repeats) can be packaged into capsids of a variety of AAV serotypes, thereby generating hybrid recombinant AAVs. At least 11 naturally occurring different AAV serotypes have been identified [11–13]. The various capsids confer different cellular specificity characteristics and also alter the time of onset of transgene expression [14,15]. We developed a method of delivering hybrid AAVs to murine otocyst progenitor cells and used this approach to identify particular AAVs capable of infecting progenitor cochlear hair cells and supporting cells.

One significant disadvantage of using AAV is that the viral genome can accommodate only a relatively small 4.8-kb gene insert [16]. To evaluate a vector with a larger capacity, we also studied the cochlear transduction characteristics of an HIV-based lentivirus pseudotyped with vesicular stomatitis virus glycoprotein (VSVG). Like AAV, if warranted, the envelope of lentivirus can be further modified to optimize cellular specificity of transduction [14,15].

Recently, it was reported that AAV2/1 and 2/2 can be used to transduce cochlear explants obtained from embryonic day (E) 15 and P0 mice. In those *in vitro* studies, transduction efficiencies of 43 and 36% were observed using AAV serotypes 1 and 2, respectively [4]. In the present study, we take these results one step further by evaluating the transduction efficiency of these and other AAV serotypes and of lentivirus after *in vivo* delivery to hair cell progenitors. Further, we evaluated those viruses found to have favorable transduction characteristics for evidence of developmental and/or functional toxicity. The results indicate that AAV2/1 has favorable transduction characteristics with respect to developing cochlear hair cells and supporting cells.

Results

Ex Utero Microinjections

Our collection of high-titer viral preps of rAAV serotypes 2/1, 2/2, 2/5, 2/7, 2/8, and 2/9 and the lenti-VSVG vector allowed us to screen a wide array of recombinant vectors. We injected many embryos (a minimum of 10 per group; see Table 1) to determine the tissue tropism for each viral serotype. We performed a midline laparotomy incision and dissected through the peritoneum, which allowed access to the uterus, which we advanced through the abdominal incision (Fig. 1A). We isolated the amniotic sacs (and placentas) surrounding the developing embryos and oriented them to reveal the left otocyst (Fig. 1B), which we then injected using glass microinjection pipettes (Fig. 1A). We used common anatomical landmarks of the E11–12.5 embryo to determine the approximate position of the otocyst. In the sagittal profile of the embryo's head, the otocyst is bounded superiorly by the inferior wall of the fourth ventricle and inferiorly by the anterior and posterior divisions of the cardinal veins (Fig. 1B). These three structures form an inferiorly pointing triangle. The injection site (Fig. 1C) is at the apex of the triangle, just beneath the most superficial tissue layer. We deemed filling of the otocyst to be complete when fast green dye, a constituent of the virus buffer, took on a keyhole-shaped appearance representative of complete filling of the hollow otocyst and the superiorly developing endolymphatic duct (Fig. 1D).

Using these techniques, we tested lenti-VSVG and our array of AAV serotypes expressing enhanced green fluorescent protein (eGFP) under a cytomegalovirus (CMV) promoter. Our initial screening showed consistent transduction of both hair cells and supporting cells within 1 week (at P0) using AAV2/1 and AAV2/8 (Figs. 2A and 2B). We saw no evidence of transgene expression in those embryos injected with AAV2/5, 2/6, 2/7, and 2/9 (Fig. 2D; Table 1). In the lentivirus-injected samples, we used an anti-GFP antibody to enhance eGFP visualization. We noted eGFP expression not in hair cells, but in other epithelial precursors of the organ of Corti (Fig. 2C). We did not study AAV2/2 with *ex utero* microinjections because our previous experience with this virus indicated that it takes several weeks after infection before transgene expression is observed. Importantly, serial sections through the heads/necks of these animals provided no evidence of transgene expression in extracochlear or extravestibular sites after delivery of any of these viruses (data not shown).

We further characterized the transduction characteristics of the vectors that appeared to be promising in *ex utero* studies (AAV2/1, AAV2/8, and lentivirus) through additional studies involving *trans*-uterine injection. This latter approach, which eliminates the need for cesarean section and cross-fostering, significantly increases the survival rates of the newborn, *in utero*-injected pups. This allowed us to examine both the long-term expression of eGFP and its distribution throughout mature cells of the cochlear and vestibular systems, as well as the potential effects of the surgery and virus exposure on normal hearing.

Trans-uterine Microinjections

Compared to *ex utero* injections, long-term survival was enhanced using *trans*-uterine injections. This was not due to differences in injection success, as similar numbers of pups survived to gestation in both groups (Table 1). The difference was due to the higher rate of

cannibalism of pups born via cesarean section and then cross-fostered (data not shown). At postnatal age 4–5 weeks, the *trans*-uterine-injected pups were sacrificed and their temporal bones were harvested for either cochlear whole mounts or midmodiolar cross sections. For those pups injected with AAV2/1, we consistently observed highly efficient and strong inner hair cell (IHC) and outer hair cell (OHC) transduction (Fig. 3A,Table 1). For lentivirus, we observed a low level of expression of eGFP in OHCs (Fig. 3B) and supporting cells (inset, Fig. 3B), but no green fluorescence in IHCs. Whole-mount microscopy of cochleas injected with AAV2/8 revealed only occasional green IHCs, OHCs, and supporting cells. Interestingly, eGFP levels derived from AAV2/8 injection were low at 4–5 weeks in comparison to what we had seen soon after injection. Examination of modiolar cross sections from AAV2/8-injected animals and comparison with OHC and IHC counts from whole-mount sections showed normal organ of Corti morphology and a normal complement of hair cells in the AAV2/1, AAV2/8, and lenti-GFP-injected 4- to 5-week-old cochleas. This is consistent with the auditory brain stem response (ABR) measures (discussed later), which demonstrated normal hearing thresholds from these same animals.

We also studied transgene expression mediated by AAV2/2. Our previous experience injecting AAV2/2 *in vivo* in the retina had shown that transgene expression begins weeks after injection [15,17]. Therefore, AAV2/2 was not part of our initial P0 screening. Previous *in vitro* studies of cochlear explants have shown AAV2/2 expression in both hair cells and supporting cells [4]. We observed rare infection (1–2 cells per cochlea) of either hair cells or supporting cells in cochlear whole mounts and modiolar cross sections 6 weeks after *trans*-uterine microinjection (in postnatal 5-week-old animals; data not shown).

To screen our samples further, we examined modiolar cross sections injected with each viral type (Figs. 3D and 3E). For those cochleas injected with AAV2/1, we again observed a classic pattern of green OHCs and IHCs (Fig. 3D). We also observed transduced supporting cells (Fig. 3D). These modiolar cross sections showed normal organ of Corti morphology. Again, for AAV2/8, we saw green fluorescent OHCs and IHCs in only a handful of hair cells per cochlea (Fig. 3E). Further, we observed no transduction of other nonsensory cells in the organ of Corti from either AAV2/1 or AAV2/8. Utricular hair cells also displayed patchy collections of green fluorescent hair cells and supporting cells for AAV2/1 and 2/8 (Figs. 3F and 3G). Yellow colabeling is seen here, and in other images, at the level of the cuticular plate. Additionally, confocal Z series with three-dimensional reconstructions of our whole mounts are available online as supplemental material.

Given that our initial studies showed AAV2/1 to be our most highly efficient and promising vector, we quantified the transduction efficiency of the virus for both IHCs and OHCs in the apical and basal turns using whole-mount preparations of the organ of Corti. We did not quantify supporting cells, but they appeared to be transduced in proportions similar to those seen with OHCs. Previous *in vitro* studies have shown a difference between expression levels in the apical and basal turns of the cochlea. Our results showed highly efficient transduction of both inner and outer hair cells throughout the cochlea (Table 1). We measured that on average, 81 and 64% of IHCs and OHCs, respectively, expressed eGFP throughout the entire cochlea.

Effects of *in Utero* Cochlear Infection on Hearing at Adulthood

To identify any toxicity of the cochlear gene transfer procedure with respect to auditory function, we measured the hearing thresholds of each injected mouse prior to sacrificing them at 4–5 weeks of age. This time point falls within a window of normal hearing for BALB/c mice. Prior to 3 weeks of age, their hearing has not fully matured. After several months of age, however, these mice begin to display age-related hearing loss. Thus, we defined 4–5 weeks of age as the ideal time point against which we could measure any gene-transfer-related hearing loss. We used the ABR as an objective measure of hearing threshold. Tone burst stimuli at four different frequencies were presented to cover a large portion of the range of mouse hearing. We observed a statistically significant difference among the groups ($P < 0.001$, ANOVA, $F = 15.608$, $df = 4$, $n = 46$). A multiple comparison (Tukey) test showed that a mild hearing loss in the lentivirus-injected group (Table 2, Fig. 4) accounted for the significance. The hearing sensitivity of the animals injected with AAV serotypes did not differ significantly from that of controls (Table 2, Fig. 4).

Discussion

There are a number of genetic and environmental diseases that affect the cochlea early in life, including mutations in genes such as connexin 26 and Atoh1. Additionally, there are genetic diseases such as Usher syndrome, which can cause blindness, deafness, and also defects in balance [3,18,19]. Expression and toxicity data suggest that treatment for these diseases would be most effective if administered early in life—in many cases, prior to differentiation of cochlear sensory structures.

In the mouse, differentiation of hair cells and supporting cells occurs in the last week of gestation and is complete within days after birth. It would thus be necessary to target defects affecting differentiation of these cells through *in utero* gene transfer. *In utero* gene therapy has been demonstrated to be effective at preventing or reversing congenital disease in animal models of a diverse set of diseases including Leber congenital amaurosis [20], mucopolysaccharidosis I [21], glycogen storage (Pompe) disease [22], hemophilia [23,24], and Crigler– Najar syndrome [25].

In comparison to other tissues, virus-mediated gene transfer to the developing otocyst has several advantages. Only small quantities of vector are necessary to fill the hollow E11–12.5 otocyst. This gives the vector efficient access to the whole complement of prosensory progenitor cells. Further, the fact that virus is delivered into an enclosed space minimizes exposure of other parts of the body. In support of this, we demonstrated that transgene expression was localized to the cochlea, with no spread to surrounding structures or the brain.

To evaluate the transduction characteristics of AAV and lentivirus–VSVG vectors, we used both an *ex utero* and a *trans*-uterine approach. These techniques allow for accurate and reproducible gene transfer to the developing murine cochlea. We have identified a window from E11 to E12.5 when microinjections into the otocyst can be performed with high survival rates. At this stage of development, the cochlear turns are just beginning to form and the hair cells are on the cusp of differentiation. Our results demonstrate that particular

hybrid AAV vectors efficiently transduce prosensory progenitor cells in a stable fashion following direct injection of virus. In addition to resulting in efficient transduction, AAV2/1 results in rapid onset of transgene expression in progenitor cells and stable expression in the mature inner and outer hair cells and their supporting cells. Further, exposure to AAV2/1 (and the other AAV serotypes that were tested) did not interfere with auditory function. Therefore, AAV2/1-mediated gene transfer should be useful not only for gene replacement/knockdown in congenital hearing diseases, but also for diseases that are acquired and require long-term gene expression. Interestingly, the AAV serotype for which the most preclinical and clinical data exist (AAV2/2) does not efficiently transduce prosensory progenitors in our hands, at least in the time frame that was evaluated.

An unexpected finding was the significantly decreased hearing in mice that were treated with lentivirus–VSVG *in utero*, despite the high percentage of OHCs expressing (low levels of) eGFP. The only explanation for this finding, given that the surgical techniques were identical, is that lentivirus–VSVG or some other component in the vector preparation has an ototoxic effect on the developing auditory system. Of note, our initial studies with lentivirus demonstrated that it was the only viral prep that infected cells other than hair cells or their adjacent supporting cells. Further, the purity of lentivirus preparations is not as high as with AAV preparations and so we cannot at present exclude a contaminant. Nevertheless, no significant contamination was evident from an evaluation of protein gels. Future studies will determine whether ototoxicity correlates with the dose of virus and/or with exposure to the VSVG protein. If the VSVG protein results in ototoxicity, the lentivirus can be pseudotyped with alternative proteins that may, in addition, have more favorable cochlear transduction characteristics [15].

In summary, we have identified a viral vector (AAV2/1) that targets cochlear prosensory progenitor cells efficiently and results in stable, early onset transgene expression. This establishes the framework for somatic gene transfer experiments, which can be used to delineate the developmental mechanisms responsible for cochlear hair cell and supporting cell differentiation. This vector can also be used to deliver therapy in animal models of congenital cochlear disease. The latter possibility is particularly attractive as there are, at present, a number of genetic models of cochlear disease. In some of these, there is concurrent retinal degeneration (i.e., Usher syndrome models), which can potentially be corrected simultaneously using *in utero* or postnatal retinal gene transfer [14,20]. Of course, there is a long series of steps (ranging from efficacy studies to safety studies to discussion of ethical implications) that must be taken before *in utero* gene therapy for human cochlear (or retinal) disease becomes a reality. Nevertheless, the results from the present study indicate that *in utero* treatment of a congenital disease causing hearing loss is indeed possible.

Materials and Methods

Virus production

The transgene cassette in all viruses consisted of CMV-driven eGFP. AAV (serotypes 2/1, 2/2, 2/5, 2/6, 2/7, 2/8, and 2/9) was prepared by triple transfection by the Medical Genetics Vector Core facility at University of Pennsylvania, as previously described (1×10^{13} genomic copies/ml) [15,26]. AAV2/2 was purified by heparin column chromatography. The

other vectors were purified using CsCl gradient centrifugation. Vector physical titers were assessed by real-time PCR and purity of the virus was ensured by endotoxin assay and gel electrophoresis.

Rhabdoviridae VSVG-pseudotyped HIV-based vector was generated by triple transfection of the helper packaging construct, the transfer vector, and the envelope expressor as previously described [27]. The titer of the purified virus used was $3 \times 10^{12} - 1 \times 10^{13}$. Virus aliquots were stored at −80°C and thawed prior to surgery.

Animals and virus administration

All procedures were performed in adherence with institutional and national guidelines and were approved by the local Institutional Animal Care and Use Committee. Four- to six-week-old animals were obtained from The Jackson Laboratory (Bar Harbor, ME, USA) and used to generate the fetuses that were injected. Timed matings were performed with noon of the plug date considered to be E0.5. After a 12-day gestational period, E12–E12.5 dams were used for fetal gene transfer. Approximately 50 nl of $3 \times 10^{12} - 1 \times 10^{13}$ genomic copies/ml virus were delivered unilaterally to the cochlea. Contralateral cochleas were uninjected and served as controls.

Ex utero microinjection

E12–E12.5 dams were anesthetized with 9 mg/ml Nembutal at 7 μl/g body wt. The abdomen was depilated and a sterile field was prepared. Using a dissecting microscope, a 1.5-cm midline laparotomy incision was made, allowing access to the uterus (Fig. 1A). Following transverse incision of the uterus, the amniotic sacs (and placentas) surrounding the developing embryos were isolated and oriented to reveal the left otocyst (Fig. 1B). Excess embryos were removed for space purposes, so that between three and six embryos remained for injection. Pressure microinjection into the otocyst was accomplished with glass needles connected to compressed nitrogen and a Harvard Apparatus (Holliston, MA, USA) PLI-100 pressure injector. Four microliters of $3 \times 10^{12} - 1 \times 10^{13}$ virus was mixed with 2 μl 0.25% fast green dye (Sigma, St. Louis, MO, USA) and aspirated into micropipettes crafted from borosilicate glass capillary tubes. Micropipettes were pulled on a David Kopf Instruments 700C pipette puller (DKI, Tujunga, CA, USA) to achieve a 18-to 20-μm outer tip diameter. The micropipettes were then beveled on a Sutter Instruments BV-10 beveler (Sutter Instruments, Novato, CA, USA) at a 28° angle. For microinjection, common anatomical landmarks of the E11–12.5 embryo were used to determine the approximate position of the otocyst (Fig. 1B). After all embryos had been injected, they were returned to the peritoneal cavity and incisions were closed.

Ex utero sample preparation

Seven days after the surgical procedure (E20/P0), the pregnant dams were sacrificed by cervical dislocation and a cesarean section was performed to harvest the pups. To evaluate transduction characteristics, the P0 pups were decapitated, and their heads were fixed in 4% paraformaldehyde (PFA)/phosphate-buffered saline (PBS) for 1 day. Heads were sagittal hemisected, postfixed, cryoprotected in 30% sucrose/PBS, and cryoembedded in optimal cutting temperature compound (OCT) (Fisher Scientific, Pittsburgh, PA, USA). The

hemiheads were then cryosectioned (Reichert Jung 8200, Leica, Germany) at 10 μm. Serial sections were collected and then analyzed with a Leica DMRE microscope (Leica Microsystems, Inc., Wetzlar, Germany) equipped with epifluorescence. Images were captured with a Hamamatsu digital camera and Openlab 2.2 image analysis software (Improvision, Inc., Boston, MA, USA). Images and figures were constructed in Adobe PhotoShop and Illustrator (Adobe Systems Inc., San Jose, CA, USA).

Trans-uterine microinjection

The methods for *trans*-uterine microinjection are identical to *ex utero* microinjection except that BALB/c mice were used instead of CBA/J mice due to easier visualization of anatomical landmarks through the uterus. Injections were *trans*-uterine and transillumination identified anatomical landmarks of the otocyst. Dams were allowed to give birth vaginally and to nurse their young to maturity.

Auditory brain-stem response testing

Mice were anesthetized (0.5 mg/kg, ip, Avertin; Sigma) and placed in a custom head holder located in a sound attenuating chamber (IAC, New York, NY, USA). Prior to the ABR recording, sound pressure at the entrance to the external auditory meatus was calibrated for every subject at each stimulus frequency with a probe tube microphone (Type 4133; Bruel & Kjaer, Denmark) and a spectrum analyzer (SR770, FFT network analyzer; Stanford Research Systems, Sunnyvale, CA, USA). ABR recordings were collected from subdermal electrodes placed at the left mastoid prominence (active electrode), vertex (reference electrode), and rump (ground electrode).

Stimulus generation and response recordings were made and analyzed using the TDT System II signal processing package (Tucker Davis Technology, Gainesville, FL, USA). Tone bursts with a duration of 4 ms (1 ms rise/fall, 2 ms plateau, 50-ms intervals) were presented at a rate of 20/s in a free field with a digital-to-analog converter connected to an electrostatic speaker. The stimulus intensity was controlled via an electronically programmable attenuator over a 90-dB range. The digitized electrical responses were amplified (100,000×) and filtered via a two-step process. Initial amplification of 1000× was made using a preamplifier with a 10- to 10,000-Hz filter (DAM-6A Differential Pre-amp, World Precision Instruments, Sarasota, FL, USA) with a secondary amplification of 100× and a 0.3- to 3-kHz filter by the TDT System II spike conditioner. Responses were recorded over a 10-ms interval, which began at the onset of the tone burst and had a 20-kHz sampling rate. Single traces whose voltage exceeded a normal level were rejected as artifact derived from muscle and cardiac activity. Approximately 500 nonartifact responses were collected and averaged at each stimulus intensity. Thresholds were defined as half the interval between the lowest stimulus intensity producing a replicable response waveform and the stimulus intensity below which no reproducible response was elicited.

Sample preparation

Following ABR testing, anesthetized mice were perfused with PFA, and the temporal bone containing the cochlea and vestibular organs was isolated. For modiolar cross sections, samples were decalcified in 120 mM ethylene diamine tetraacetic acid for 24 h and then

cryoprotected. The samples were embedded in OCT with each block containing one to three injected cochlea and one uninjected contralateral negative control oriented in the lower right section of the block. After cryosectioning in the midmodiolar plane, the sections were stained with a 1:20 dilution of an anti-myosin VIIa primary antibody (Novus Biologicals, Littleton, CO, USA) followed by a 1:200 dilution of a TRITC-conjugated secondary antibody (Molecular Probes, Carlsbad, CA, USA). Sections containing eGFP-positive hair cells were then stained with a 1:200 dilution of phalloidin 633 antibody (Molecular Probes), which stains F-actin [28]. Selected slides were also stained with a 1:600 dilution of anti-eGFP antibody (Molecular Probes) followed by a 1:200 dilution of a FITC-conjugated secondary antibody (Molecular Probes) to enhance low levels of eGFP fluorescence. We limited this staining to those samples infected with lentivirus, as these consistently demonstrated a low level of eGFP expression.

Transduction efficiency protocol

Cochlea specimens used for hair cell counting and whole-mount immunofluorescence were not decalcified. Apical and basal cochlear turns were stained with a 1:200 dilution of phalloidin antibody as above. Whole-mount samples were then mounted on glass slides for analysis using a Zeiss laser scanning confocal microscope and software (Zeiss, Germany). Images of the organ of Corti were taken using two channels. The red channel was used to count the total number of hair cells in each image stained with phalloidin, while the green channel was used to count the number of cells in each image that expressed eGFP. Three-dimensional reconstructions were created with Volocity software (Improvision Ltd., Lexington, MA, USA).

Supplementary Material

Refer to Web version on PubMed Central for supplementary material.

Acknowledgments

This study was supported by NIH R01 EY10820 (J.B.), NIH R01 DC006442 02 (M.A.G.), T32 DC005363 03 (J.C.B.), and 5-P30-DK-47747-10 (Vector Core Facility); the Foundation Fighting Blindness (J.B.); the Lois Pope LIFE Foundation (J.B.); the William and Lew R. Wasserman Merit Award (J.B.); Research to Prevent Blindness, Inc.; the Paul and Evanina Mackall Trust; and the F. M. Kirby Foundation. We also thank Daniel Chung, Tonia Rex, Jeannette Bennicelli, Zhangyong Wei, and Aatish Patel (University of Pennsylvania) for technical assistance.

References

1. Lalwani A. Development of in vivo gene therapy for hearing disorders: introduction of adeno-associated virus into the cochlea of the guinea pig. Gene Ther. 1996; 3:588–592. [PubMed: 8818645]
2. Zine A. Molecular mechanisms that regulate auditory hair-cell differentiation in the mammalian cochlea. Mol Neurobiol. 2003; 27:223–237. [PubMed: 12777689]
3. Izumikawa M, et al. Auditory hair cell replacement and hearing improvement by Atoh1 gene therapy in deaf animals. Nat Med. 2005; 11:271–276. [PubMed: 15711559]
4. Stone I, Lurie D, Kelley M, Poulsen D. Adeno-associated virus-mediated gene transfer to hair cells and support cells of the murine cochlea. Mol Ther. 2005; 11:843–848. [PubMed: 15922954]
5. Han J, et al. Transgene expression in the guinea pig cochlea mediated by a lentivirus-derived gene transfer vector. Hum Gene Ther. 1999; 10:1867–1873. [PubMed: 10446926]

6. Derby M, Sena-Esteves M, Breakefield X, Corey D. Gene transfer into the mammalian inner ear using HSV-1 and vaccinia virus vectors. Hear Res. 1999; 134:1–8. [PubMed: 10452370]
7. Praetorius M, et al. A novel vestibular approach for gene transfer into the inner ear. Audiol Neurootol. 2002; 7:324–334. [PubMed: 12463195]
8. Lalwani A, Walsh B, Carvalho G, Muzyczka N, Mhatre A. Expression of adeno-associated virus integrated transgene within the mammalian vestibular organs. Am J Otol. 1998; 19:390–395. [PubMed: 9596192]
9. Luebke A, Steiger J, Hodges B, Amalfitano A. A modified adenovirus can transfect cochlear hair cells in vivo without compromising cochlear function. Gene Ther. 2001; 8:789–794. [PubMed: 11420643]
10. Luebke A, Foster P, Muller C, Peel A. Cochlear function and transgene expression in the guinea pig cochlea, using adenovirus- and adeno-associated virus-directed gene transfer. Hum Gene Ther. 2001; 12:773–781. [PubMed: 11339894]
11. Gao GP, Alvira M, Wang L, Calcedo R, Johnston J, Wilson J. Novel adeno-associated viruses from rhesus monkeys as vectors for human gene therapy. Proc Natl Acad Sci USA. 2002; 99:11854–11859. [PubMed: 12192090]
12. Rutledge E, Halbert C, Russell D. Infectious clones and vectors derived from adeno-associated virus (AAV) serotypes other than AAV type 2. J Virol. 1998; 72:309–319. [PubMed: 9420229]
13. Mori S, Wang L, Takeuchi T, Kanda T. Two novel adeno-associated viruses from cynomolgus monkey: pseudotyping characterization of capsid protein. Virology. 2004; 330:375–383. [PubMed: 15567432]
14. Surace E, et al. Delivery of adeno-associated viral vectors to the fetal retina: impact of viral capsid proteins on retinal neuronal progenitor transduction. J Virol. 2003; 77:7957–7963. [PubMed: 12829835]
15. Auricchio A, et al. Exchange of surface proteins impacts on viral vector cellular specificity and transduction characteristics: the retina as a model. Hum Mol Genet. 2001; 10:3075–3081. [PubMed: 11751689]
16. Dong J, Fan P, Frizzell R. Quantitative analysis of the packaging capacity of recombinant adeno-associated virus. Hum Gene Ther. 1996; 7:2101–2112. [PubMed: 8934224]
17. Bennett J, Duan D, Engelhardt JF, Maguire AM. Real-time, noninvasive in vivo assessment of adeno-associated virus-mediated retinal transduction. Invest Ophthalmol Visual Sci. 1997; 38:2857–2863. [PubMed: 9418740]
18. Oshima K, Heller S. Sound from silence. Nat Med. 2005; 11:249–250. [PubMed: 15746932]
19. Ahmed Z, Riazuddin S, Riazuddin S, Wilcox E. The molecular genetics of Usher syndrome. Clin Genet. 2003; 63:434–444.
20. Dejneka N, et al. Fetal virus-mediated delivery of the human RPE65 gene rescues vision in a murine model of congenital retinal blindness. Mol Ther. 2004; 9:182–188. [PubMed: 14759802]
21. Meertens L, et al. In utero injection of alpha-L-iduronidase-carrying retrovirus in canine mucopolysaccharidosis type I: infection of multiple tissues and neonatal gene expression. Hum Gene Ther. 2002; 13:1809–1820. [PubMed: 12396614]
22. Rucker M, et al. Rescue of enzyme deficiency in embryonic diaphragm in a mouse model of metabolic myopathy: Pompe disease. Development. 2004; 131:3007–3019. [PubMed: 15169761]
23. Schneider H, et al. Sustained delivery of therapeutic concentrations of human clotting factor IX—A comparison of adenoviral and AAV vectors administered in utero. J Gene Med. 2002; 4:46–53. [PubMed: 11828387]
24. Waddington S, et al. In utero gene transfer of human factor IX to fetal mice can induce postnatal tolerance of the exogenous clotting factor. Blood. 2003; 15:1359–1366. [PubMed: 12393743]
25. Seppen J, van der Rijt R, Looije N, van Til N, Lamers W, Oude Elferink R. Long-term correction of bilirubin UDPglucuronyltransferase deficiency in rats by in utero lentiviral gene transfer. Mol Ther. 2003; 8:593–599. [PubMed: 14529832]
26. Hildinger M, Auricchio A, Gao G, Wang L, Chirmule N, Wilson J. Hybrid vectors based on adeno-associated virus serotypes 2 and 5 for muscle-directed gene transfer. J Virol. 2001; 75:6199–6203. [PubMed: 11390622]

27. Mochizuki H, Schwartz J, Tanaka K, Brady R, Reiser J. High-titer human immunodeficiency virus type 1-based vector systems for gene delivery into nondividing cells. J Virol. 1998; 72:8873–8883. [PubMed: 9765432]

28. Holt J. Functional expression of exogenous proteins in mammalian sensory hair cells infected with adenoviral vectors. J Neurophysiol. 1999; 81:1881–1888. [PubMed: 10200223]

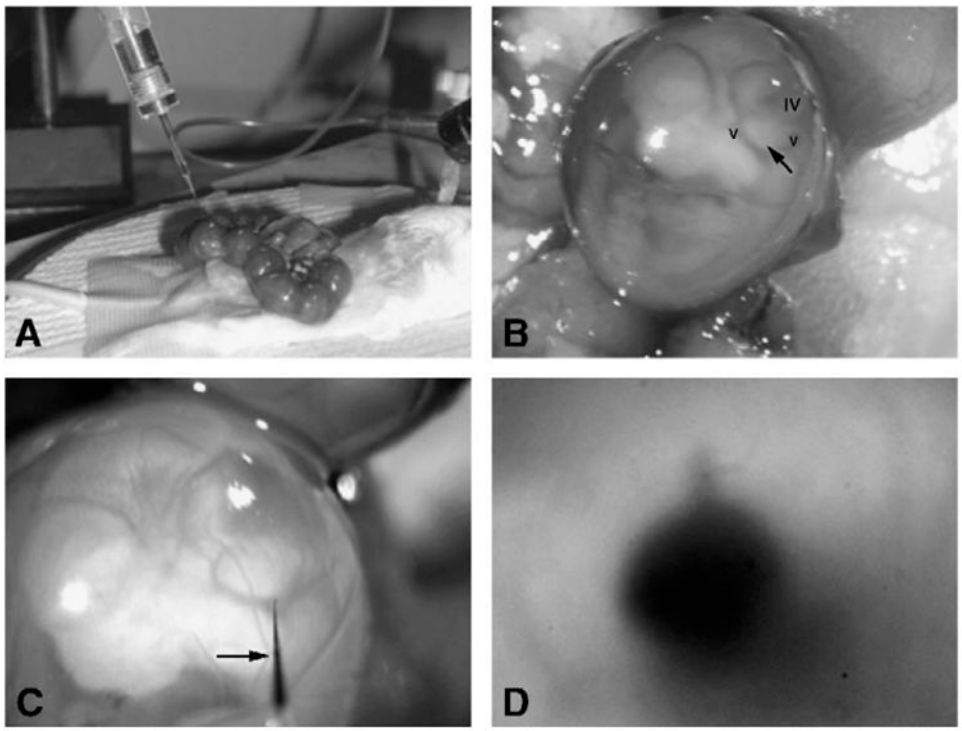

Fig. 1.

Methods of *ex utero* and *trans*-uterine microinjection. The surgical setup of the *trans*-uterine approach is shown as viewed through the dissecting microscope. (A) The uterus is exposed and the fetuses appear as a “string of beads” following midline laparotomy. (B) The left sagittal profile of the embryo at E12. Visible are the cardinal veins (v) and fourth ventricle (iv). The closed arrow points to the otocyst and the injection spot. (C) The microinjection pipette enters the amniotic sac (closed arrow). The light refracts the pipette tip as it enters the amniotic fluid. (D) After injection, dye is visible in the otocyst. Note the keyhole-shaped filled endolymphatic duct protruding away from the otocyst at the 12 o'clock position.

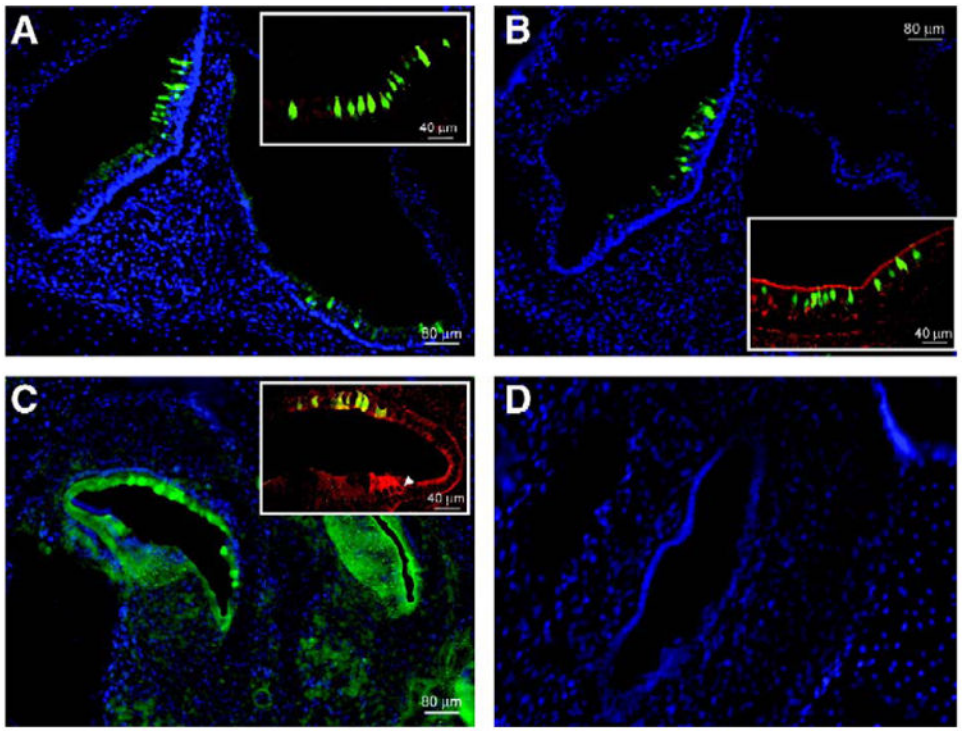

Fig. 2.

Sagittal cryosections of the murine cochlear and vestibular systems. eGFP-expressing hair cells and supporting cells are seen with fluorescence microscopy in cochlear and vestibular sagittal cryosections of P0 mice that had been injected at E12. (A) Vestibular section after exposure to AAV2/1 (original magnification 10×). The inset (original magnification 25×) shows transduced hair cells and supporting cells that express eGFP. Anti-myosin VIIa antibody is used as a hair cell marker and the reactive cells appear red. Hair cells that express eGFP as well as myosin VIIa appear green-yellow at the colocalization sites. (B) AAV2/8-injected cryosections are seen at 10× original magnification with a 25× original magnification inset. (C) Cochlear section after exposure to lentivirus and staining with an anti-eGFP antibody followed by FITC for better visualization. The white arrow in the inset indicates a myosin VIIa-stained hair cell. Nonspecific eGFP colocalization with this stain appears yellow-green. (D) Nuclei (stained blue with DAPI) outline the macula in the utricle in a sample from an AAV2/9-injected mouse. eGFP is absent.

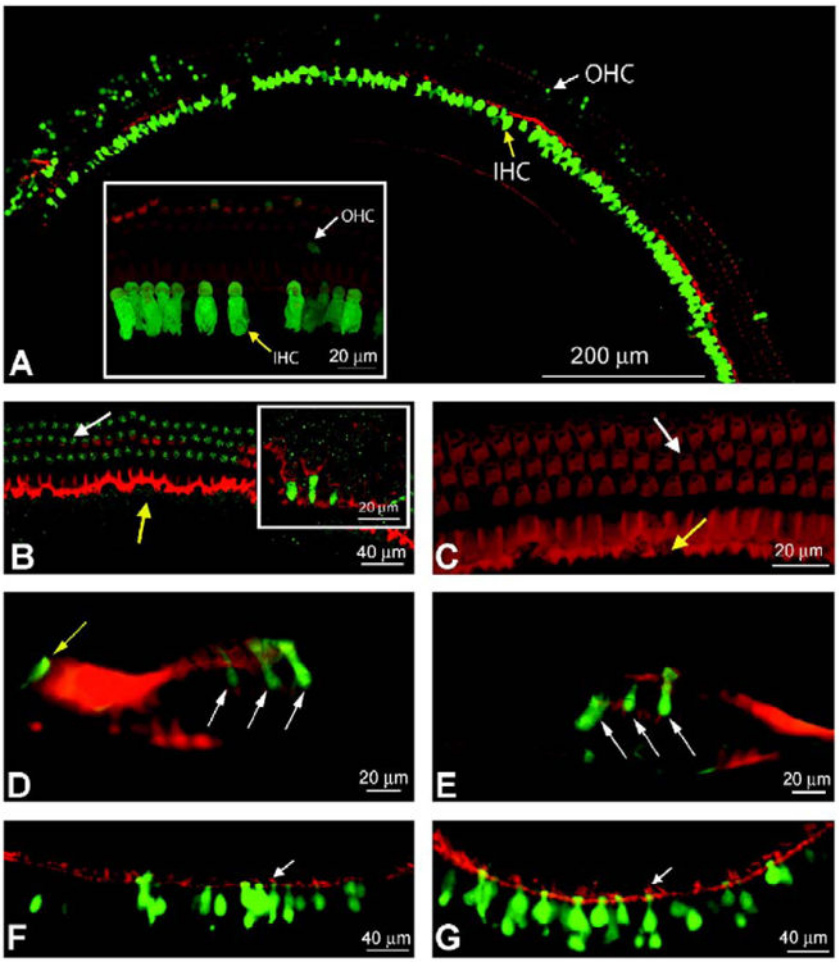

Fig. 3.

Long-term gene expression in IHCs and OHCs. Confocal images of mature cochleae after *in utero* microsurgical viral injection. (A) A composite image of an apical turn is seen under confocal microscopy at original magnification 25×. Phalloidin, which stains F-actin in hair cells and supporting cells, appears red. A fragment of the cochlear turn is seen at original magnification 63× in the inset, which shows inner and outer hair cells that were transduced and express eGFP. Both images are of a cochlea injected with AAV2/1. White arrows mark OHCs and yellow arrows indicate transduced IHCs. (B) A segment of apical turn from a cochlea injected with lentivirus is seen at original magnification 25×. Three rows of OHCs are observed with a low level of eGFP expression. No IHCs are expressing eGFP. A 63× original magnification inset shows green fluorescent supporting cells indicating viral transduction. (C) A confocal projection image from an uninjected negative control at original magnification 63×. It is stained with phalloidin and exposed at a gain similar to that of the cochlear turn in (B) to demonstrate staining above background in (B). (D and E) AAV2/1- and 2/8-injected modiolar cross sections, respectively, at original magnification 40× are seen under light microscopy. The white arrows indicate infected OHCs and the yellow arrow indicates an infected IHC. (F and G) AAV2/1- and 2/8-injected utricular sections are seen at original magnification 20× under light microscopy. Many green

fluorescent hair cells and supporting cells are observed. White arrows point to hair cell stereociliae as an indicator of hair cells. In several images, the cuticular plate can be distinguished by its yellow colabeling.

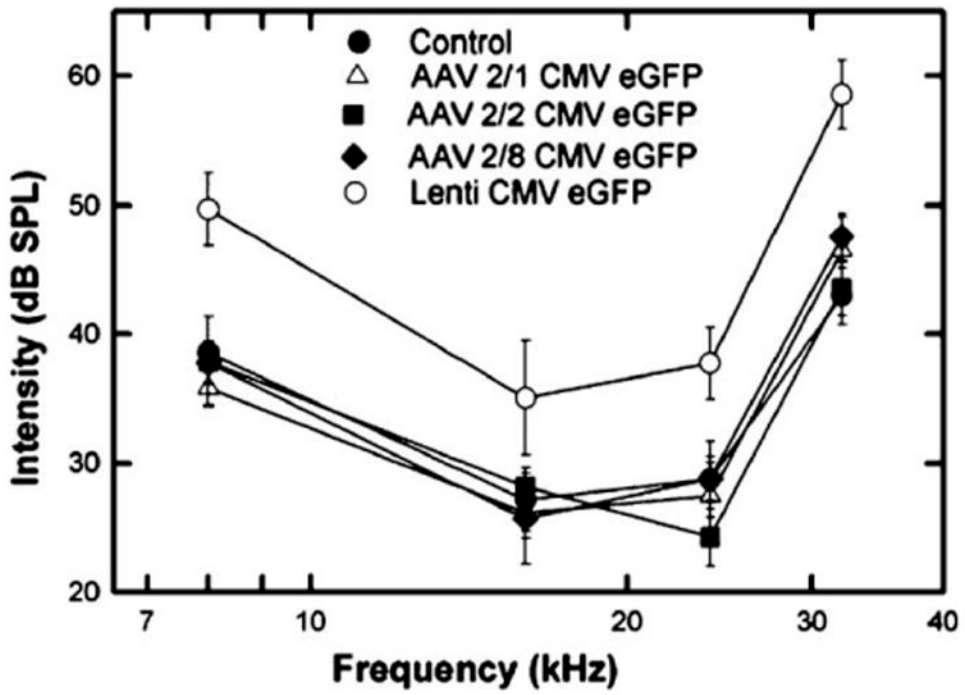

Fig. 4.

ABR responses in adult mice following *in utero*gene transfer. Average ABR thresholds in decibels referenced to sound pressure level (dB SPL) are plotted against frequency for groups of mice injected *in utero* with each viral vector. Frequencies tested were 8, 16, 24, and 32 kHz. Standard error of the mean ranges are plotted for each data point. A statistically significant threshold shift at each of the frequencies is seen between the lentiviral-injected mouse group and the uninjected controls ($P < 0.001$). No statistically significant difference between the rAAV-injected groups and controls was observed.

Table 1

Microsurgical injections and transduction efficiencies

	P0 post-*ex utero* injections			E12–12.5 *trans*-uterine injections			Average hair cell transduction efficiency of AAV2/1		
	Dams	Live pups	Infected hair cells	Dams	Live pups at 5 weeks	Infected hair cells		IHCs	OHCs
AAV2/1	5	16 (72%)	+++	6	1 7 (63%)	++++	Total	81.42%	64.03%
AAV2/2	0	NA	N/A	2	9 (100%)	+	Apical turn	82.54%	63.70%
AAV2/5	2	7 (78%)	–				Basal turn	79.40%	64.67%
AAV2/6	2	7 (78%)	–						
AAV2/7	2	10 (100%)	–						
AAV2/8	4	6(31%)	+++	6	21 (78%)	+			
AAV2/9	2	4 (44%)	–						
Lentivirus	3	10(71%)	+	5	1 3 (59%)	++			

Listed are the numbers of pregnant dams operated on and the subsequent numbers of live pups born that had been injected with each viral serotype. Numbers in parentheses indicate the percentages of injected fetuses that survived birth. On the first postnatal day qualitative assessments of the rate of hair cell infectivity, demonstrated by eGFP expression, were made. (+++) Highest infectivity rates. (–) No infectivity. Based on these data, *trans*-uterine microinjections of selected AAV serotypes and lentivirus were performed for longer term studies. Shown in the middle columns are the numbers of pregnant dams operated on and numbers of live injected pups from those dams after 5 weeks. Qualitative assessment of hair cell infection was again noted. Of the pups infected with AAV2/1, whole mounts were made of the apical and basal cochlear turns for hair cell counting to assess viral transduction efficiency.

Mol Ther. Author manuscript; available in PMC 2014 July 23.

Table 2

ABR thresholds

		Average ABR threshold (dB SPL)								Controls vs injected
No. of mice tested		**8 kHz**	**SEM**	**16 kHz**	**SEM**	**24 kHz**	**SEM**	**32 kHz**	**SEM**	***P* values**
5	Controls	38.6	0.9	27.2	2.5	28.7	2.9	43.0	2.2	N/A
10	AAV2/1	35.7	1.3	26.2	2.0	27.4	2.6	46.5	2.6	1.000
9	AAV2/2	37.9	3.5	28.2	1.5	24.3	2.2	43.5	6.2	0.995
11	AAV2/8	37.8	1.6	25.7	3.5	28.8	1.7	47.5	1.9	0.999
11	Lentivirus	49.7	2.9	35.1	4.4	37.7	2.8	58.5	2.7	<0.001

Auditory brain-stem response (ABR) thresholds in decibels sound pressure level (dB SPL) with associated standard errors of the mean for each of four pure tone frequencies are shown. Only the lentivirus group shows a statistically significant difference ($P < 0.001$) from control ABR thresholds.

Mol Ther. Author manuscript; available in PMC 2014 July 23.